Asymptotic structure of charged colloids between two and three dimensions: the influence of salt

2008 J. Phys.: Condens. Matter 20 494232

(http://iopscience.iop.org/0953-8984/20/49/494232)

J. Phys.: Condens. Matter **20** (2008) 494232 (6pp) doi:10.1088/0953-8984/20/49/494232

Asymptotic structure of charged colloids between two and three dimensions: the influence of salt

Sabine H L Klapp[1,3], **Stefan Grandner**[1], **Yan Zeng**[2] **and Regine von Klitzing**[2]

[1] Institut für Theoretische Physik, Sekretariat EW 7-1, Technische Universität Berlin, Hardenbergstraße 36, D-10623 Berlin, Germany
[2] Stranski-Laboratorium für Physikalische und Theoretische Chemie, Sekretariat TC 9, Technische Universität Berlin, Straße des 17. Juni 124, D-10623 Berlin, Germany

E-mail: sabine.klapp@fluids.tu-berlin.de

Received 28 July 2008
Published 12 November 2008
Online at stacks.iop.org/JPhysCM/20/494232

Abstract
We present theoretical, computer simulation and experimental results for the structural length scales characterizing bulk and confined charged colloidal suspensions. The target quantities are the bulk pair correlation functions on the one hand, and the oscillatory solvation forces of the colloids in films of various thicknesses on the other. Recently we have shown, for a system with very low salt concentration, that these quantities are characterized by the same wavelength in the asymptotic limit, in agreement with predictions from density functional theory. Here we consider systems with larger ionic strengths of added salt. Our results indicate that the wavelength remains essentially unaffected, whereas the correlation length and the amplitude depend significantly on the amount of added salt. Indeed, already at ionic salt strengths as low as 10^{-3} mol l^{-1} the force oscillations essentially disappear.

1. Introduction

Confining fluids in slit-pore geometries leads to damped oscillatory surface forces [1]. This well-known effect is directly related to the oscillatory density profile perpendicular to the surface [2, 3]. The oscillation period indicates the distance between regions of high density, that is, the layers formed parallel to the confining surface. The decay length is a measure of how far the surfaces must be separated to observe homogeneous bulk-like behavior in between. Oscillatory forces are a rather generic feature occurring for atomic and molecular fluids, but also for colloidal particles [4–8], liquid crystals [9] and aggregates such as micelles and polyelectrolytes [10–14]. These complex confined fluids can also be considered as solvents ('depletion agents'). The layering of the solvent particles then induces oscillations in the resulting depletion interactions [15–17].

Understanding these interactions and the behavior of the underlying confined solvent is essential in colloid science, e.g. to ensure stability against flocculation, in biological contexts (e.g., stacking of red blood cells) and, generally, for the design of novel materials and devices for micro- and nanofluidics. A particularly interesting question in this context is the relation between the structural observables in confined geometry (solvation force, depletion potential) and the structure in the corresponding bulk system.

Recently we have started to address these questions for a system which is treatable both by experiment and by theory [18, 19]. Specifically, a charged colloidal suspension composed of silica nanospheres was considered. In [19] we have analyzed one key quantity characterizing the oscillatory forces, that is, the wavelength. In particular, we have shown that this quantity coincides with the wavelength characterizing the *asymptotic* behavior of the bulk correlation function at the same chemical potential (and temperature). In this way, we have verified predictions from density functional theory (DFT), where the above relation is well-established [20, 21]. The results in [19] were obtained for one particular ionic strength. The purpose of the present work is to present theoretical and experimental data illustrating the impact of an increasing salt concentration on the wave and correlation length.

[3] Author to whom any correspondence should be addressed.

2. Experiments

2.1. Materials

Ludox grade TMA colloidal silica beads (LUDOX TMA-34 deionized) were used as nanoparticles. The suspension was purchased from Aldrich (Taufkirchen, Germany). In order to remove the salt the samples were dialyzed against Milli Q water (Millipore, Billerica, USA) for 10 days. The tubes, with a molecular weight cut off of 1000, were from Roth (Karlsruhe, Germany). A diameter of 25 ± 2 nm was determined by scanning electron microscopy (SEM), small angle neutron scattering (SANS) and scanning force microscopy (SFM). The ζ-potential is about -80 mV at an ionic strength below 10^{-5} mol l^{-1}, determined by a Nanozetasizer (Malvern).

After dialysis, the particle weight concentration was determined by weighting the suspensions before and after drying in an oven (24 h at 400 °C). Suspensions at concentrations between 5 and 17 wt% were prepared with Millipore water. The volume concentration of particles can be converted by the particle density (2.2 g ml^{-1}) and density of original TMA suspension (1.2 g ml^{-1}). The ionic strength was adjusted by adding a known amount of NaCl solution (Carl Roth GmbH & Co.).

2.2. Colloidal probe atomic force microscopy (CP–AFM)

The colloidal probe technique was invented by Ducker *et al* [22]. In our experiments, a silica particle of radius $R = 3.31$ μm was used as the colloidal probe. It was glued with epoxy (UHU Plus Endfest 300) to a tipless cantilever (Ultrasharp Contact Silicon Cantilevers, CSC12) produced by μMasch and distributed by Anfatec. The colloidal probes were purchased from Bangs Laboratories, Inc. The tip was cleaned by plasma cleaning for 10 min just before each measurement cycle to remove all the organic components on its surface. The substrate was a silicon wafer with a native SiO_2 top layer, cleaned by the RCA method [23] and stored in Millipore water before use. Just before each experiment, the substrate was taken out of the water and dried in a nitrogen stream. Drops of the Ludox particle suspension were spread onto the substrate and the probing head immersed in the solution droplet. Force versus distance curves ($F(h)$) were measured with a commercial atomic force microscope molecular force probe (MFP) produced by Asylum Research, Inc. and distributed by Atomic Force (Mannheim, Germany). The scanning frequencies of approaching–retreating runs were 0.1 Hz for distances of 100–500 nm. Since the distance between the colloidal probe and the substrate is much smaller than the diameter of the colloidal probe, by Derjaguin approximation, the curved surface of the colloidal probe can be considered as a flat surface and the interaction energy per area $E(h)$ can be acquired from the force $F(h)$, $E(h) = F(h)/2\pi R$. As both the Ludox particles and the SiO_2 surfaces are negatively charged, there is generally no adsorption of particles onto the surfaces. For each suspension 30–40 force–distance curves were measured at different lateral positions on the same substrate as well as on different substrates to ensure reproducibility and to get good statistics. The oscillatory forces are fitted according to the equation

$$\frac{F}{2\pi R} = A_{\mathrm{f}} \exp\left(-\frac{h}{\xi_{\mathrm{f}}}\right) \cos\left(2\pi \frac{h}{\lambda_{\mathrm{f}}} + \theta_{\mathrm{f}}\right) + \text{offset}, \qquad (2.1)$$

where F is the force, R is the radius of the colloidal probe and h is the distance between the substrate and the colloidal probe, i.e. the thickness of the liquid film between the two solid surfaces. The three important parameters that characterize the oscillation are the amplitude A, the decay length ξ_{f} and the period λ_{f}. In the discussion that follows, the phase shift θ_{f} and the offset are omitted for the sake of clarity. In fitting the force data, we have neglected the region close to hard contact, which is discussed below. The final result for each parameter is the average of 10–20 fitting results and the error bar is from the standard deviation.

3. Theoretical methods

We model the suspension on an effective level via the electrostatic part of the Derjaguin–Landau–Verwey–Overbeek (DLVO) potential [24] involving only the negatively charged silica macroions. The resulting interaction reads

$$u(r) = \tilde{Z}^2 e_0^2 \frac{\exp(-\kappa r)}{4\pi\epsilon_0\epsilon r}, \qquad (3.1)$$

where e_0 is the elementary charge, ϵ_0 and ϵ are the permittivity of the vacuum and the solvent dielectric constant, respectively, and $\tilde{Z} = Z\exp(\kappa\sigma/2)/(1+\kappa\sigma/2)$ is an effective valency involving the inverse Debye screening length $\kappa = (e_0^2/\epsilon_0\epsilon k_{\mathrm{B}}T)^{1/2}(Z\rho + 2IN_{\mathrm{A}})^{1/2}$ (with ρ being the particle number density). Here, I is the ionic strength of the added salt, and we set the valency $Z = 35$ and $\sigma = 26$ nm [18]. In addition to the DLVO potential, the particles interact (for numerical reasons) via soft-sphere repulsion; the strength of this interaction, however, is negligible compared with the DLVO repulsion (of about 50 $k_{\mathrm{B}}T$) at typical interparticle distances.

To calculate the bulk correlation function $g_{\mathrm{b}}(r)$ of our model we have performed canonical Monte Carlo (MC) simulations using $N = 500$–2000 particles depending on the volume fraction $\Phi = (\pi/6)\rho\sigma^3$. In addition, we have numerically solved integral equations for $g_{\mathrm{b}}(r)$ consisting of the exact Ornstein–Zernike equation combined with the approximate hypernetted chain (HNC) closure [25]. A convenient feature of using integral equations is that the *asymptotic* structure, that is, the dominant wave and correlation length of the function $h_{\mathrm{b}}(r) = g_{\mathrm{b}}(r) - 1$ (with $h_{\mathrm{b}}(r)$ being the total correlation function) in the limit $r \to \infty$ can be determined directly. This is done via an analysis of the complex poles $q = \pm q_1 + \mathrm{i}q_0$ of the structure factor $S_{\mathrm{b}}(q) = 1 + \rho\tilde{h}_{\mathrm{b}}(q)$ [20]. The pole with the smallest imaginary part then determines the slowest exponential decay and thus the asymptotic behavior of $h_{\mathrm{b}}(r)$, i.e.

$$r h_{\mathrm{b}}(r) \to A_{\mathrm{b}} \exp(-q_0 r)\cos(q_1 r - \theta_{\mathrm{b}}), \qquad r \to \infty, \qquad (3.2)$$

with q_0 playing the role of an inverse correlation length, that is, $q_0 = \xi_{\mathrm{b}}^{-1}$, and $q_1 = 2\pi/\lambda_{\mathrm{b}}$ determining the wavelength

λ_b of the oscillations. At the state points considered all poles have both a real and an imaginary part, in agreement with earlier findings for Yukawa-like systems [26]. We have also determined q_0 and q_1 from the MC data by plotting the function $\ln(r|h_b(r)|)$. Wavelength and correlation length then follow from the oscillations and the slope of the straight line connecting the maxima at large r.

The slit-pore confinement is modeled by two plane parallel, smooth, uncharged surfaces separated by a distance h along the z-direction and of infinite extent in the x–y plane. The fluid–wall potential $u_{fw}(z)$ is chosen to be purely repulsive and decays as z^{-9} [18]. This simple choice is motivated by the fact that, according to DFT arguments [21], the precise shape of $u_{fw}(z)$ should influence only the fluid's behavior close to the wall but not the *asymptotic* decay of the solvation pressure and related quantities. To investigate the confined systems we have employed MC simulations in the grand canonical (GC) ensemble, that is, at constant temperature, wall separation, box area parallel to the walls, and constant chemical potential μ [18, 27]. Furthermore, the inverse Debye length was fixed at the value corresponding to the bulk volume fraction.

The key quantity extracted from the GCMC calculations is the normal ('solvation') pressure, $f(h) = P_{zz}(h) - P_b$, where P_b is the pressure of the bulk system at the same chemical potential, and $P_{zz}(h)$ can be calculated as a statistical average involving the instantaneous normal component of the (virial) pressure tensor [27]. According to density functional predictions, the *asymptotic* behavior of $f(h)$ should be governed by the same wave and correlation (decay) length as the bulk pair correlation function (see (3.2)), that is

$$f(h) \to A_w \exp(-q_0 h)\cos(q_1 h - \theta_w), \qquad h \to \infty, \quad (3.3)$$

with $q_0 = \xi_f^{-1}$ and $q_1 = 2\pi/\lambda_f$ having the same values as in the bulk (see (3.2)). In other words, DFT predicts that $\xi_f = \xi_b$ and $\lambda_f = \lambda_b$. Indeed, our previous simulations and experiments [18, 19] have explicitly confirmed the second prediction, indicating that the wavelength is not affected by the fluid–wall interactions. On the other hand, the amplitude A_w and phase θ_w depend on the nature of fluid–wall interactions [21, 28]. Our numerical (GCMC) results for $f(h)$ (see section 4) show that (3.3) with $q_0 = \xi_b^{-1}$ and $q_1 = 2\pi/\lambda_b$ indeed provides a very good description for the asymptotic decay of the normal pressure of the present charged systems. Specifically, we use (3.3) for wall separations $h > h_{min}$, where h_{min} corresponds to the first minimum in the normal pressure. For smaller wall separations we use a cubic polynomial:

$$f(h) = a_0 + a_1 h + a_2 h^2 + a_3 h^3, \qquad h < h_{min}. \quad (3.4)$$

The coefficients are adjusted such that both the pressure and its derivative are continuous at h_{min}. Then, having found an accurate fit formula for $f(h)$ one may immediately integrate $f(h)$ [16][4] to obtain the solvation force $F(h)/2\pi R$.

[4] The size ratio between the microsphere (diameter $2R$) used in the CP-AFM experiment and that of a silica sphere (diameter σ) is $\sigma/2R \approx 7\times10^{-4}$, which justifies Derjaguin's approximation here [16].

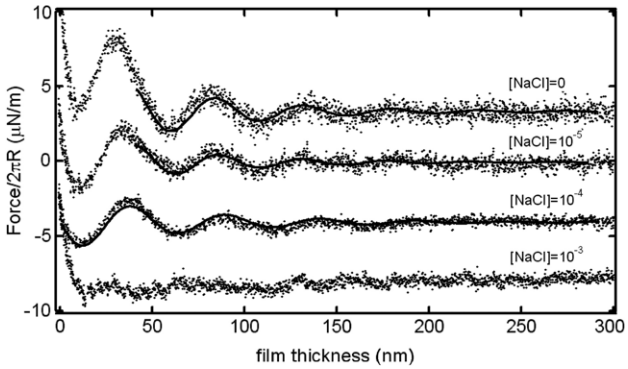

Figure 1. Experimental curves for $F(h)$ obtained by CP-AFM for four different ionic strengths at $\Phi = 7$ vol% (the data have been vertically offset for clarity). The ionic strengths were adjusted by addition of NaCl as indicated (I is given in mol l^{-1}). The solid lines are fits according to (2.1).

4. Results and discussion

Our main goal in this paper is to identify the effect of the ionic strength, I, on the surface force and solvation pressure and the related bulk properties.

As a starting point we consider in figure 1 experimental results for $F(h)$ from CP-AFM measurements at the volume fraction $\Phi = 7$ % and four different ionic strengths obtained by adding zero, 10^{-5}, 10^{-4} and 10^{-3} mol l^{-1} NaCl to the system. It is seen that the force amplitude decreases significantly with increasing ionic strength. Moreover, even at a NaCl concentration of 10^{-3} mol l^{-1} the oscillations in the force have essentially disappeared. Similar results were obtained for confined polyelectrolyte solutions where the oscillations were drastically reduced after adding salt well below the ionic strength induced by the polyelectrolytes [29].

The solid lines in figure 1 are the fitting curves obtained according to (2.1). The fit describes the experimental curves at distances larger than one or two oscillations quite well, but not on shorter length scales. We note in this context that, according to (3.3) and (3.2), the expression (2.1) describes only the *asymptotic* behavior of the oscillatory force. That means, the breakdown of (2.1) at small h is rather expected. In addition, the deviation from the fit at shorter lengths could be due to crystallization effects close to the surface. Interestingly, the deviation from the asymptotic behavior at small h becomes less pronounced with increasing ionic strength. This behavior may indicate that the increasing electrostatic screening within the system lowers the tendency for ordering and/or crystallization at the surface.

Simulation results for the functions $f(h)$ at $\Phi = 7\%$ are shown in figure 2(a). Included are the corresponding fit functions (see section 3) and the resulting structural forces $F(h)/2\pi R$. According to all these data, the primary effect of adding salt consists in a pronounced decrease of the amplitude of the oscillations. This is consistent with the experimental data for $F(h)$. Indeed, also within the GCMC simulations the oscillations essentially vanish at $I \approx 10^{-3}$ mol l^{-1}. For the smaller ionic strengths considered in figure 2(a) the oscillatory asymptotic decay of $f(h)$ is very well described by the leading

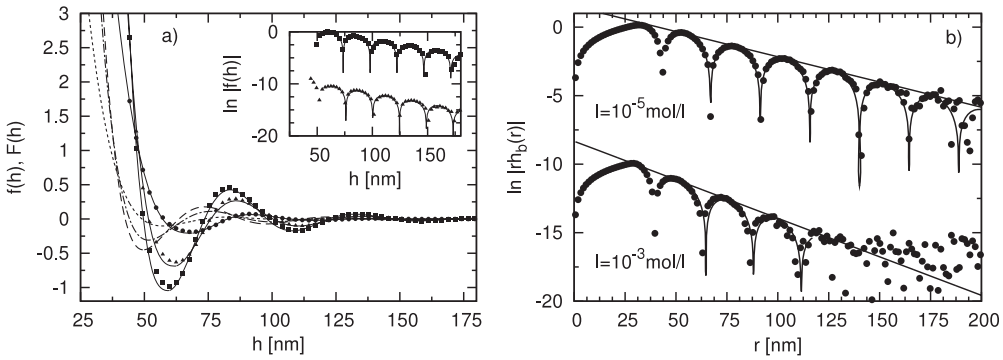

Figure 2. (a) Solvation pressure $f(h)$ as obtained by GCMC at $\Phi = 7$ % and three different ionic strengths (filled boxes, $I = 10^{-5}$ mol l^{-1}; triangles, $I = 10^{-4}$ mol l^{-1}; circles, $I = 5 \times 10^{-4}$ mol l^{-1}). Also shown are the corresponding fit functions (solid lines) obtained from (3.3) and (3.4) and the resulting structural forces $F(h)/2\pi R$ (dashed and dotted lines). Note that $f(h)$ has been fitted using the bulk values for wave and correlation length, λ_b and ξ_b. (b) Corresponding MC data for the bulk function $\ln(r|h_b(r)|)$. The asymptotic fit functions obtained from (3.2) are plotted as solid lines.

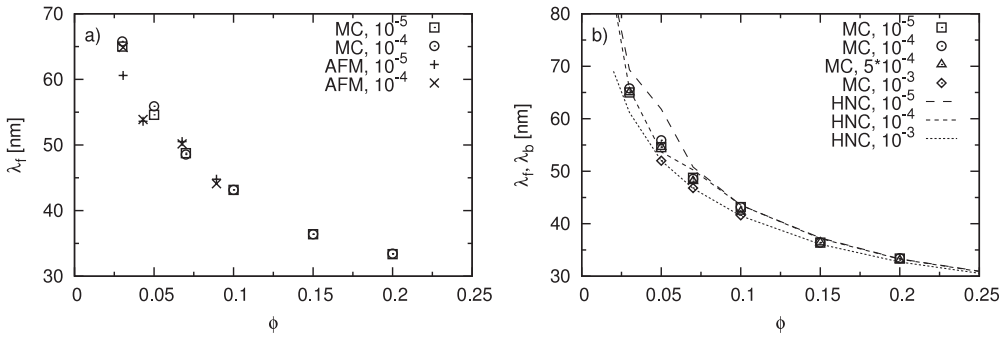

Figure 3. Asymptotic wavelength as function of the volume fraction for different ionic strengths I (in mol l^{-1}). (a) MC simulation results (where $\lambda_f = \lambda_b$) and experimental data from CP-AFM measurements. (b) MC and HNC results for the bulk system.

bulk wave and correlation lengths λ_b and ξ_b characterizing the MC bulk correlation functions, as already mentioned in section 3. This is consistent with the DFT predictions [21] and also with earlier numerical findings by the authors [19] for systems at low I. Moreover, the asymptotic expression for $f(h)$ given in (3.3) is found to provide a good approximation of the oscillations even at remarkably small wall separations, that is, around the first minimum in $f(h)$ at $h \approx 2\sigma = 52$ nm. Results for the bulk correlation functions are plotted in figure 2(b) together with the resulting asymptotic fit from (3.2). Even without a more detailed analysis one observes from the logarithmic plot in figure 2(b) a decrease of the slope of $\ln(r|h_b(r)|)$ towards more negative values, that is, a decrease of the correlation length ξ_b, with increasing salt concentration. This is consistent with the damping of oscillations observed in $f(h)$ in figure 2(a).

Comparing directly the theoretical and experimental force–distance curves, respectively, one observes pronounced differences with respect to amplitudes and the range of the oscillations. We note that differences are indeed expected in view of the simplified fluid–wall potential $u_{fw}(z)$ used in our theoretical calculations. More precisely, according to DFT [21], only the wavelength and decay length determining the *asymptotic* behavior should be independent of $u_{fw}(z)$, whereas amplitudes and phases (that is, the distance where the asymptotic behavior actually sets in) should strongly depend on the model details.

We now consider in more detail the influence of the ionic strength on the wavelength λ_f determining the oscillations of the solvation force. Experimental CP-AFM results for λ_f as a function of the silica volume fraction and two ionic strengths (where oscillations could be observed at all) are plotted in figure 3(a). Also shown are MC data for λ_f which, as explained above, equal the bulk wavelength λ_b. Furthermore, we have included in figure 3(b) HNC results for λ_b obtained from a pole analysis of the corresponding bulk correlation function. Various observations can be made. First, each of the three approaches (CP-AFM, MC, HNC) consistently predicts that variation of the ionic strength has only a very small effect on the actual value of λ. In particular, differences between $I = 10^{-5}$ and $I = 10^{-4}$ mol l^{-1} are essentially negligible. Only at $I = 10^{-3}$ mol l^{-1} (where the oscillations in the experiment had already disappeared), do the results indicate a slight decrease of the wavelength compared to smaller values of I. This decrease is in qualitative agreement with earlier HNC calculations [18] for the *average* wavelength obtained from the location of the main peak of the structure factor. Quantitatively, however, the salt dependence of the structure-factor wavelength [18] is more pronounced than that of the asymptotic wavelength displayed in figure 3(b).

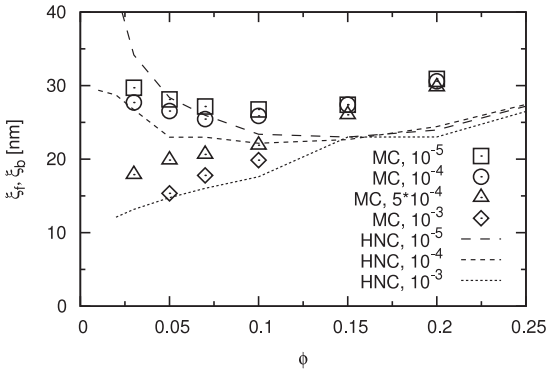

Figure 4. MC and HNC results for the bulk correlation length as function of the volume fraction for different ionic strengths I (in mol l^{-1}). Within the MC simulations, $\xi_f = \xi_b$.

Secondly, we see from figure 3(a) that there is excellent agreement between experimental and MC simulation data for λ_f. This is a strong evidence that the actual shape of the fluid–wall interactions is *irrelevant* for the period of the force, which conforms with the DFT predictions. Moreover, comparing the MC and HNC results (see figure 3(b)) we conclude that these two theoretical approaches are in good agreement.

Thirdly, all three approaches predict a power-law behavior of the wavelength according to $\lambda \propto \Phi^{-b}$ with $b \approx 1/3$, corresponding to an isotropic ordering. Thus, although the system is confined and characterized by layer formation (i.e. translational symmetry is broken), the average interparticle separation along the direction normal to the surface remains the same as in the isotropic bulk phase.

Finally, we address the asymptotic correlation (decay) lengths, ξ_f, of the oscillatory surface forces. Regarding the theoretical results, we have found (as for the wavelength) that the MC values ξ_f in confined geometry equal those in the bulk system, ξ_b. Having this is mind, we plot in figure 4 the MC results for ξ_b as a function of the volume fraction for different values of I. For comparison we have included (bulk) HNC data. Both approaches predict a significant influence of the ionic strength on the correlation length as long as the volume fraction is not too large, that is, $\Phi \leqslant 15\%$. For smaller volume fractions, adding salt at a fixed silica concentration yields a pronounced decrease of ξ_b, in agreement with what we have already seen in figure 2. This can be explained by simple screening arguments. Interestingly, the actual density dependence of ξ_b also depends on the ionic strength, that is, on κ (see (3.1)). For $I \geqslant 5 \times 10^{-4}$ mol l^{-1}, ξ_b increases monotonically with Φ in the range of volume fractions considered. These strongly screened systems behave more like systems with hard repulsive potentials (such as hard spheres) where the range of oscillatory correlations (and thus, ξ_b) just increases with Φ. On the other hand, for $I \leqslant 10^{-4}$ mol l^{-1}, we observe an initial decrease of ξ_b with a minimum at $\Phi \approx 10\%$. This different behavior may be interpreted as follows. For small values of I and Φ, increasing the silica concentration has a similar effect to adding salt since both yield an increase of the inverse Debye length κ, and thus the screening. This leads, in turn, to a damping of oscillations in the bulk correlations and the related surface properties. Only at larger Φ does the system with low salt behave again like a 'hard-sphere' in that ξ_b increases with Φ. From figure 4 it is seen that these trends of the correlation length are predicted both by the (quasi-exact) MC data and by HNC theory. However, the latter seems to strongly overestimate both the impact of I and the resulting density dependence at small concentrations.

The experimentally determined decay (correlation) lengths have large error bars. However, at all densities considered the average value of ξ_f is larger than the theoretical correlation lengths plotted in figure 4. This is also visible in the slower decay of the experimental force curves (see figure 1) in comparison to the simulated ones (see figure 2). According to DFT, the different fluid–wall potential in experiments and theory should not have any effect on ξ_f, as long as the *asymptotic* limit is considered. However, particularly in the experimental data, there is clearly some uncertainty regarding the separation h where the asymptotic behavior actually sets in. Further investigations of the correlation length and its density and salt dependence are under way.

Acknowledgments

Financial support from the German Science Foundation via the Sfb 448 'Mesoscopically structured composites' (projects B6 and B10) and from the Fonds der Chemischen Industrie is gratefully acknowledged. Furthermore, we are indebted to Wacker Siltronic AG for providing the silicon wafers.

References

[1] Israelachvili J N and Pashley R M 1983 *Nature* **306** 249
[2] Chaudhury M K 2003 *Nature* **423** 131
[3] Wasan D T and Nikolov A D 2003 *Nature* **423** 156
[4] Piech M and Walz J Y 2002 *J. Colloid Interface Sci.* **253** 117
[5] Tulpar A, van Tassel P R and Walz J Y 2006 *Langmuir* **22** 2876
[6] Jönsson B, Broukhno A, Forsman J and Akesson T 2003 *Langmuir* **19** 9914
[7] Kittner M and Klapp S H L 2007 *J. Chem. Phys.* **126** 154902
[8] Jordanovic J and Klapp S H L 2008 *Phys. Rev. Lett.* **101** 038302
[9] Ivanov I B and Dimitrov D S 1988 *Thin Liquid Films* ed I B Ivanov (New York: Dekker) p 379
[10] Stubenrauch C and von Klitzing R 2003 *J. Phys.: Condens. Matter* **15** R1197
[11] von Klitzing R, Kolaric B, Jaeger W and Brandt A 2002 *Phys. Chem. Chem. Phys.* **4** 1907
[12] von Klitzing R and Tieke B 2004 *Polyelectrolytes with Defined Molecules Architecture I* (*Series: Advances in Polymer Science* vol 165) ed M Schmidt (Heidelberg: Springer) p 177
[13] McNamee C E, Tsujii Y, Ohshima H and Matsumoto M 2004 *Langmuir* **20** 1953
[14] Qu D, Pedersen J S, Garnier S, Laschewsky A, Möhwald H and von Klitzing R 2006 *Macromolecules* **39** 7364
[15] Bechinger C, Rudhardt D, Leiderer P, Roth R and Dietrich S 1999 *Phys. Rev. Lett.* **83** 3960
[16] Götzelmann B, Evans R and Dietrich S 1998 *Phys. Rev.* E **57** 6785
[17] Roth R, Evans R and Dietrich S 2000 *Phys. Rev.* E **62** 5360
[18] Klapp S H L, Qu D and von Klitzing R 2007 *J. Phys. Chem.* B **111** 1296

[19] Klapp S H L, Zeng Y, Qu D and von Klitzing R 2008 *Phys. Rev. Lett.* **100** 118303
[20] Evans R, Henderson J R, Hoyle D C, Parry A O and Sabeur Z A 1993 *Mol. Phys.* **80** 755
[21] Grodon C, Dijkstra M, Evans R and Roth R 2005 *Mol. Phys.* **103** 3009
[22] Ducker W A, Senden T J and Pashley R M 1991 *Nature* **353** 239
[23] Kern W 1984 *Semicond. Int.* **94** 94–9
[24] Verwey E J W and Overbeek J T G 1948 *Theory of Stability of Lyophobic Colloids* (Amsterdam: Elsevier)
[25] Hansen J P and McDonald I R 2006 *Theory of Simple Liquids* 3rd edn (Amsterdam: Academic)
[26] Hopkins P, Archer A J and Evans R 2005 *Phys. Rev.* E **71** 027401
[27] Schoen M and Klapp S H L 2007 Nanoconfined fluids: soft matter between two and three dimensions *Reviews of Computational Chemistry* vol 24, ed K B Lipkowitz and T Cundari (New York: Wiley)
[28] Qu D, Brotons G, Bosio V, Fery A, Salditt T, Langevin D and von Klitzing R 2007 *Colloids Surf.* A **303** 97
[29] Kolarić B, Jaeger W and von Klitzing R 2000 *J. Phys. Chem.* B **104** 5096